NASA-TM-112911

Dynamically Tuned Blade Pitch Links for Vibration Reduction

Judah Milgram
Rotorcraft Fellow

Inderjit Chopra
Professor and Director

Center for Rotorcraft Education and Research
Department of Aerospace Engineering
University of Maryland
College Park, Maryland 20742

Sesi Kottapalli

NASA Ames Research Center
Rotorcraft Aeromechanics Branch
Moffett Field, California 94035

Abstract

A passive vibration reduction device in which the conventional main rotor blade pitch link is replaced by a spring/damper element is investigated using a comprehensive rotorcraft analysis code. A case study is conducted for a modern articulated helicopter main rotor. Correlation of vibratory pitch link loads with wind tunnel test data is satisfactory for lower harmonics. Inclusion of unsteady aerodynamics had little effect on the correlation. In the absence of pushrod damping, reduction in pushrod stiffness from the baseline value had an adverse effect on vibratory hub loads in forward flight. However, pushrod damping in combination with reduced pushrod stiffness resulted in modest improvements in fixed and rotating system hub loads.

Introduction and Background

Since the early days of rotorcraft development, vibration reduction has been a central topic of research. This will continue to be the case until vibration levels comparable to those in fixed wing aircraft can consistently be achieved without excessive weight penalty. Research in rotorcraft vibration reduction techniques is motivated primarily by the need to maximise structural component life, reduce crew fatigue and provide a more comfortable environment for passengers. Also, public acceptance of helicopters as a means of transportation depends to a large degree on passenger comfort. Vibration reduction may be thus be viewed as significant to the economic success of the rotorcraft industry.

Recent research in vibration reduction has focused on two main approaches:

1. Structural optimization, i.e. structural design or modification to achieve favorable fuselage and blade dynamic characteristics.

2. Active vibration control (higher harmonic and/or individual blade control using either hydraulic actuators or smart structures technology, actively controlled fixed system actuators).

The first approach has perhaps the greatest potential for achieving low vibration levels with minimum weight penalty. Nevertheless, at present it does not appear that this approach can be relied upon to achieve desired vibration levels in every case. First, it must be recognized that vibration prediction is a complex multidisciplinary problem; existing vibration prediction analyses are not reliable enough to guarantee success of structural optimization. Second, the approach is limited to the design phase of a new aircraft. In the case of existing aircraft, structural optimization is unattractive since it will typically involve complete redesign of major structural components. Finally, the aircraft is subjected to a wide variety of loadings and operating conditions and it is difficult to arrive at an optimum design which satisfies all conditions.

Active control is also promising but has drawbacks in the form of weight penalty and additional power requirements. Also, the maintainability and relisbility aspects of active vibration control systems may make them less attractive in many applications.

A third category of vibration reduction technology is made up of discrete passive devices, such as pendular absorbers in the rotating system, antiresonance isolators for gearbox isolation, spring-mass absorbers in the fuselage, etc. Although these devices also bring a weight penalty, and in some cases increased maintenance requirements, they are in general simple, relatively inexpansive, and can applied on an as-needed

Presented at the 50th Annual Forum of the American Helicopter Society, Washington, DC, May 11-13, 1994

basis in combination with other vibration reduction measures. Thus, irrespective of technology advances in structural design methodology or active control, it will always be advantageous to have a selection of effective passive devices available. This paper examines the vibration reduction potential of one such passive device, the tuned spring-damper pushrod.

An early study by Miller and Ellis (Ref. 1) examined the effects of torsional frequency on blade root shears. A simple rigid blade model was used and the torsional frequency was varied by adjusting a root torsional spring. The model thus applies to the case of a variable stiffness pushrod. The study showed that reductions in root torsional spring stiffness could lead to substantial reductions in blade vibratory shears.

Subsequent investigators (for example, Refs. 2 and 3) examined the influence of blade torsional frequency on blade response. However, these studies were directed more towards reduction of the control system vibratory loads associated with stall flutter than to reduction of hub loads and fuselage vibration.

A spring-damper pushrod to modify blade torsional dynamics was first investigated in the early 1970's at Sikorsky Aircraft (Ref. 4), again with a goal of reducing vibratory loads in the control system arising from stall flutter. The spring and damping values were selected based on an analytic investigation of a single flight condition known to produce high stall-induced vibratory loads. The investigation culminated in a flight test of a set of spring-damper pitch links on a CH-54B helicopter. The devices were quite effective; at high speed, vibratory control loads in the rotating system were reported reduced by nearly 50%. The cockpit vibration levels were unchanged, but it is not clear whether this was based on pilot comments or on actual vibration measurements.

Recently, Kottapalli (Ref. 5) suggested that introduction of large values of torsional damping at a discrete location near the blade root could reduce blade elastic motions and vibratory hub loads. The study was conducted using a full elastic blade analysis (CAMRAD). The torsional damper was represented by applying an equivalent damping to the first torsion mode. The effects of applying the damping at a discrete location were not investigated. No specific damping device was discussed, but it is clear that tuned spring-damper pushrod such as that tested in Ref. 4 could be adapted to the purpose. This is an attractive possiblity since it replaces the conventional pushrod and therefore can be installed in both new and existing rotorcraft.

The present study further examines the possibilities for vibration reduction via pushrod tuning. Unlike the Ref. 4 study, the analysis focuses on the influence of tuning on vibratory hub shears rather than stall-induced control loads. The pushrod is represented as a discrete element and the effects of pushrod damping on the blade root boundary condition are realistically represented.

The investigation is in several parts. First, the rigid blade pitch-flap analysis of Miller and Ellis (Ref. 1) is repeated using a trimmed forward flight model. Then, a more extensive investigation with a comprehensive rotor analysis is conducted. Measured and predicted pushrod load data are compared to validate the analytic model. The effects of pushrod stiffness and damping on fixed and rotating system hub loads are examined. The study concludes with a discussion of practical considerations and suggestions for future work.

Rigid Blade Pitch-Flap Analysis

Preliminary to the actual investigation, the rigid blade pitch-flap analysis of Miller and Ellis (Ref. 1) was repeated. The goal was to gain insight into the pushrod tuning problem using a simple model, eliminating complicating factors such as blade elastic motions, pushrod kinematics and blade twist. Unlike Ref. 1, the present analysis directly includes the effects of forward flight.

The physical model (Fig. 1) is a rigid blade, free to flap and pitch about centrally located coincident hinges. The blade is restrained at the root through a torsion spring. Collective and cyclic pitch inputs are applied to the blade through the torsion spring so as to trim the rotor to a prescribed value of thrust

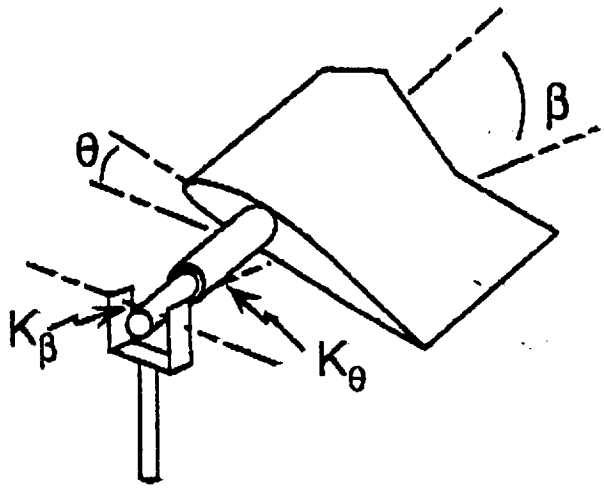

Figure 1: Rigid blade pitch-flap physical model.

and zero first harmonic flapping. The rotor shaft angle is adjusted to achieve propusive trim based on an assumed fuselage equivalent flat plate area. The flapping frequency may be adjusted with an assumed flapping hinge spring. The model assumes a flap-pitch hinge sequence and zero pitch-flap (δ_3) coupling. The equations of motion are solved with the finite element in time method, and blade root loads are computed via a force summation scheme.

The study was conducted assuming a typical blade with characteristics in Table 1. This is essentially the blade examined in Ref. 1. The first flapping frequency has been set at 1.05/rev, typical of an articulated blade with small hinge offset.

Table 1: Blade Model Parameters for Loads Data in Fig. 2

Flapping frequency	ν_β	1.05/rev
Baseline torsional frequency	ν_θ	5/rev
Lock number	γ	8
Blade chord	c/R	.05 (solidity = .0159 per blade)
CG offset	e_{cg}/R	.0005 (fwd. of feather axis)
AC offset	e_{ac}/R	.00025 (fwd. of feather axis)
Moment of inertia about feather axis	I_θ/I_β	.001
Torsional damping	ζ_θ	0
Pitch-flap coupling	δ_3	0
Profile lift curve slope	a_0	6.28
Profile lift at zero angle of attack	α_{l_0}	0
Profile pitching moment coefficient	$c_{m_{ac}}$	0
Profile drag coefficient	c_{d_0}	.01
Fuselage equivalent flat plate area	$f_e/\pi R^2$	.0025

Figure 2 shows blade root loads and fixed system hub loads as a function of torsional frequency for a coupled trim condition at $\mu = .4$. Note in this study only pushrod stiffness variations (i.e. variations in torsional frequency) are investigated. The torsional damping is set zero. In Figure 2(a), the 3/rev load shows a considerable reduction over the baseline value ($\nu_\theta = 5$) as the rotational torsional frequency approaches 3/rev. A sudden fourfold increase in the 3/rev blade vertical shear is encountered as the torsional frequency is further lowered to just under 3/rev. There is a very slight reduction in the 2/rev load local to $\nu_\theta = 3$. The 4/rev vertical load is coupled to 3/rev pitching motion due to large 1/rev variation in dynamic pressure and hence also shows a large peak at this torsional frequency. There is also a small reduction in 3/rev shear when the torsional frequency nears 4/rev. These basic features observed in the 3/rev shear are also present in the 4/rev vertical shear near $\nu_\theta = 4$ and in the blade root moment results in Fig. 2(b). The peaks in amplitude, however, are of lesser magnitude.

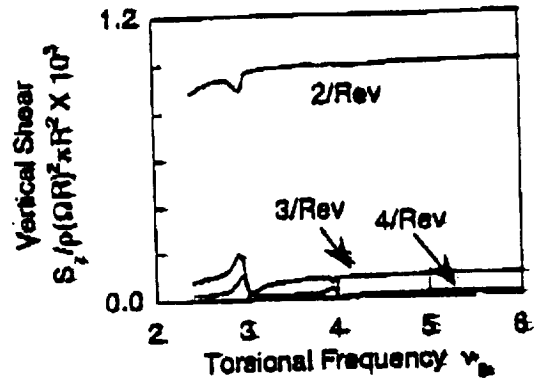

(a) Blade root vertical shears (rotating system).

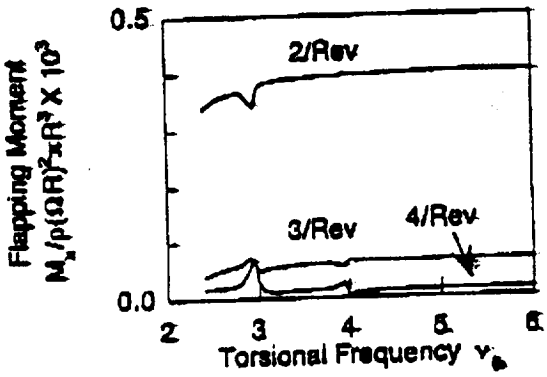

(b) Blade root bending moment (rotating system).

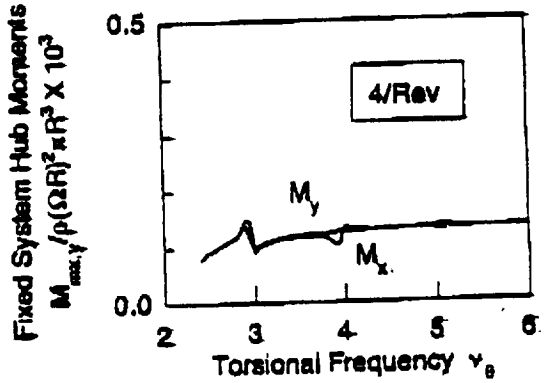

(c) Fixed system pitch and roll moments.

Figure 2: Rigid blade root and hub vibratory loads vs. blade torsional frequency. $\mu = .4$; $C_T/\sigma = .1$.

Strictly speaking, since this is a centrally hinged blade, the 3/rev vertical shears would be of interest

from a vibration point of view only with $N_b = 3$. However, with hinge offset, these vertical shears produce 3/rev rotating system hub moments contributing to fixed system moments with $N_b = 4$.

Figure 2(c) shows fixed system 4/rev hub moments, assuming a four bladed rotor. Note the values of c/R and C_T chosen for the single blade yield $C_T = .0064$ and $C_T/\sigma = .1$ for a four bladed rotor. The slight reduction in fixed system moments near $\nu_\beta = 3$ (compared with the baseline, $\nu_\beta = 5$) is due to the corresponding reduction in 3/rev rotating system loads (figure 2(b)).

It does not appear possible to identify a single combination of pitch, flap, and airloads harmonics which are responsible for the reduction in vibratory load near $\nu_\beta = 3.05$. This is a two degree of freedom system; the flapping and torsion degrees of freedom are coupled through mass, damping, and stiffness terms and both contribute to the vibratory load through inertia terms. Therefore one should not expect a simple single degree of freedom resonance phenomenon resulting in a sharp peak in response or a 90° phase shift. Indeed, the local minimum in vibration and associated side peak is reminiscent of the characteristic of a spring-mass vibration absorber (see *e.g.* Ref. 6).

Nevertheless, these results do tend to confirm the conlusion of Ref. 1 that for this rigid blade model, vibration reduction is indeed possible by proper selection of the blade torsional frequency. The optimum frequency lies just above 3/rev. The underlying effect is not a simple resonance phenomenon; the relative phasing of the various harmonics of the loads may play an important role. A vibration penalty may result from operating slightly off the design point.

Elastic blade analysis

The major part of the investigation was conducted using UMARC, a comprehensive rotor aeroelastic analysis based on finite elements in time and space (Ref. 7).

In Ref. 5, the effects of the spring/damper were represented by an equivalent modal damping of the blade first torsional mode. This approach in essence assumes that the damping is distributed uniformly over the length of the blade. Although this simplifying assumption is appropriate for a preliminary study such as Ref. 5, in the present analysis it was considered essential to model the pitch link as a discrete dynamic element applied at its proper location. The spring/damper pitch link changes the blade root boundary conditions and affects the blade root torsional dynamics in a manner that is not properly captured if a distributed damping is assumed.

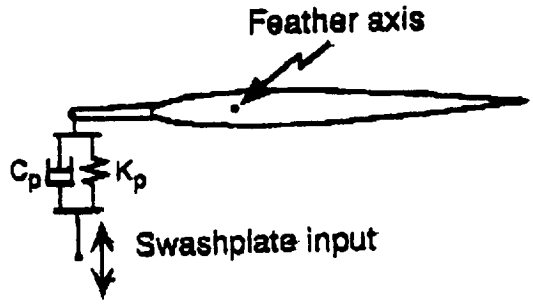

Figure 3: Spring-damper pushrod

In the present analysis the spring-damper pushrod (Fig. 3) is modeled by modifying the analysis to release the blade root boundary constraint. Appropriate energy terms are added to the stiffness and damping matrices. These include diagonal terms on the root pitch degree of freedom due to the pushrod stiffness and damping, and both diagonal and coupling terms on the blade flap degree of freedom arising from the δ_3 coupling. The pushrod motions are calculated from the control inputs and the elastic blade root pitch and flap deflections. The pushrod loads are obtained from the pushrod motions together with the known pushrod stiffness and damping values.

Validity of modal approximation with damped boundary condition

The analysis is configured to apply a modal approximation to the equations of motion. The basis of the modal reduction is the set of normal modes obtained with only the stiffness and mass terms in the equations of motion. This leads to another modeling issue, namely, how well can these undamped normal modes represent the blade dynamics in the presence of a damped boundary condition? Physically speaking, one would expect that, given enough damping, the blade root motion would be restricted to the point where a cantilever boundary condition would apply, with a corresponding increase in torsional frequency. This is the "bridging" phenomenon mentioned in Ref. 4. However, the modes obtained without the damper include deflections at the blade root and do not satisfy this boundary condition.

In Figure 4, a uniform elastic rod is supported at one end with a spring and damper arranged in parallel. Undamped normal modes for this system are calculated from the closed form solution for a spring-supported torsion rod. A set of the first N of these modes are then used to synthesize the system including the damper. The resulting modal damping matrix

is fully populated. The frequency thus calculated for the first damped torsion mode is shown in Figure 4 as a function of the root damping coefficient. In the figure the damping coefficient has been normalized to $\sqrt{GJ\mu}$ and the frequencies to $\frac{\pi}{2}\sqrt{\frac{GJ}{\mu l^2}}$, the exact solution for the cantilever case. The figure shows that above a certain value of the root damping coefficient, the predicted frequency is above that for the cantilever case. As can be expected, this overprediction becomes less severe as the number of modes is increased. However, for all the cases shown, as long as the calculated torsional frequency remains below $\omega_d/\omega_{ref} = 1$, there is relatively little sensitivity to the number of normal modes used. In the analysis to follow, the blade is represented by its first seven modes. Although this includes only one mode which can be categorised as a "pure" torsion mode, it includes two bending modes which involve significant amounts of torsional motion due to structural twist. It will be shown that this set of normal modes together with the pushrod damping values of interest result in only moderate increases in torsional frequency, and it is concluded that the error due to using undamped normal modes is insignificant.

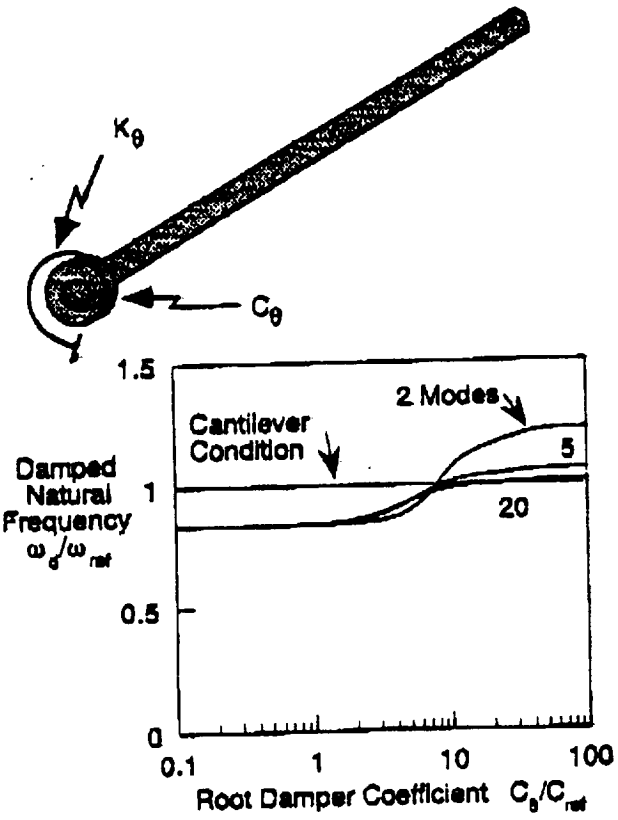

Figure 4: First torsional natural frequency of uniform rod with spring/damper boundary condition. $K_\theta GJ/l = 5$.

Results

Subject aircraft

The remainder of the paper will examine the effects of varying pushrod stiffness and damping of a typical helicopter rotor, in this case the a Sikorsky S-76. A full scale S-76 main rotor was tested in the NASA Ames 40 × 80 wind tunnel in the late 1970's (Ref. 8), providing experimental data for verification of the analytical results. The design characteristics are given in Table 2. In Ref. 8, four tip planforms were tested; the present investigation assumes the rectangular tip configuration in order to minimize modeling issues related to three-dimensional unsteady effects at the blade tip. Detailed data for the analytic model are available in Refs. 8 and 9.

The blade pushrod stiffness of the baseline aircraft is based on the control system stiffness given in Ref. 9, together with the assumption that this stiffness is entirely determined by the pushrod stiffness with no compliance to the swashplate or servos. This assumption is adequate for the present feasibility study; nevertheless, it should be borne in mind that in the actual aircraft the control system stiffness may be affected by the swashplate and servo stiffness.

According to the normalization scheme used in the present analysis (Ref. 7), the nondimensional pushrod stiffness is defined as

$$\bar{k}_p = \frac{k_\theta}{m_0\Omega^2R^3\left(\frac{e_x}{R}\right)^2}$$

Table 2: Main rotor basic design data, Sikorsky S-76 (Refs. 8 and 9)

Number of blades	N_b	4
Blade tip		Rectangular (wind tunnel test only)
Blade torsional frequency	ν_θ	5.5/rev (calculated with baseline pushrod)
Solidity	σ	.0748
Lock number (nominal)	γ	10.6
Rotor speed	Ω	30.7 1/s
Tip speed	ΩR	675 ft/s
Flap and Lag Hinge Offset	ϵ	3.8%
Blade Pitch-Flap Coupling	δ_3	17°
Pitch Bearing Torsional Stiffness	$k_{\theta_p B}$	680 ft-lb/rad
Control System Stiffness	k_θ	24000 ft-lb/rad
Pitch horn arm	e_{PH}/R	.0246

with the reference mass distribution m_0 defined as

$$m_0 = \frac{3I_\beta}{(1-\epsilon)^3 R^3}$$

This is the mass distribution which, if constant along the blade span, would yield the actual flapping moment of inertia, I_β. Based on the mass data in Ref. 9, m_0 for this blade amounts to .126 slug/ft, yielding a non-dimensional value of $\bar{k}_\beta \approx 31.2$ for the baseline aircraft

Correlation with test data

To validate the analysis, the measured pushrod load time histories from Ref. 8 are compared with the analytic results for the same operating conditions. Figures 5(a) and 5(b) compare the measured and analytic results for advance ratios of .2 and .38 respectively. In each case, the rotor is trimmed to zero first harmonic flapping and the specified C_T/σ. The data have been adjusted to zero steady component to facilitate comparison of the vibratory components of the waveforms. Two sets of analytic results are shown; first one obtained using quasisteady aerodynamic modeling, and second one using unsteady circulatory aerodynamic terms. The dynamic stall model provided as an option in the analysis was not activated.

In each case, the overall correlation with the measured data is fair At both $\mu = .2$ and $\mu = .38$, the 1/rev vibratory components appear fairly well matched. However, at $\mu = .2$, the test data exhibit a small signal at near the blade first torsional frequency which is not present in the calculated results. At $\mu = .38$, the predicted and calculated data differ noticeably in phase over the retreating portion of the rotor disk. Nevertheless, the main features of the torsional response are present in the predicted time histories, namely, the large excursion on the advancing side at near 2/rev and the presence of response at the torsional frequency on the retreating side.

Only small differences are observed in the two sets of analytic results. Hence, quasisteady aerodynamics will be used for the remainder of this study. As mentioned earlier, the optional dynamic stall model is not used in this investigation. It appears unlikely, however, that inclusion of the stall model would improve the overall correlation. Stall flutter is not a significant factor in the experimental data since the large "spikes" in pushrod load typically occuring in the aft retreating quadrant of the rotor disk (see for example Refs. 4 and 3) are entirely absent. Also, significant deviations between the measured and predicted time histories are observed near $\psi = 180°$; this is not a region on the rotor disk where stall would be expected

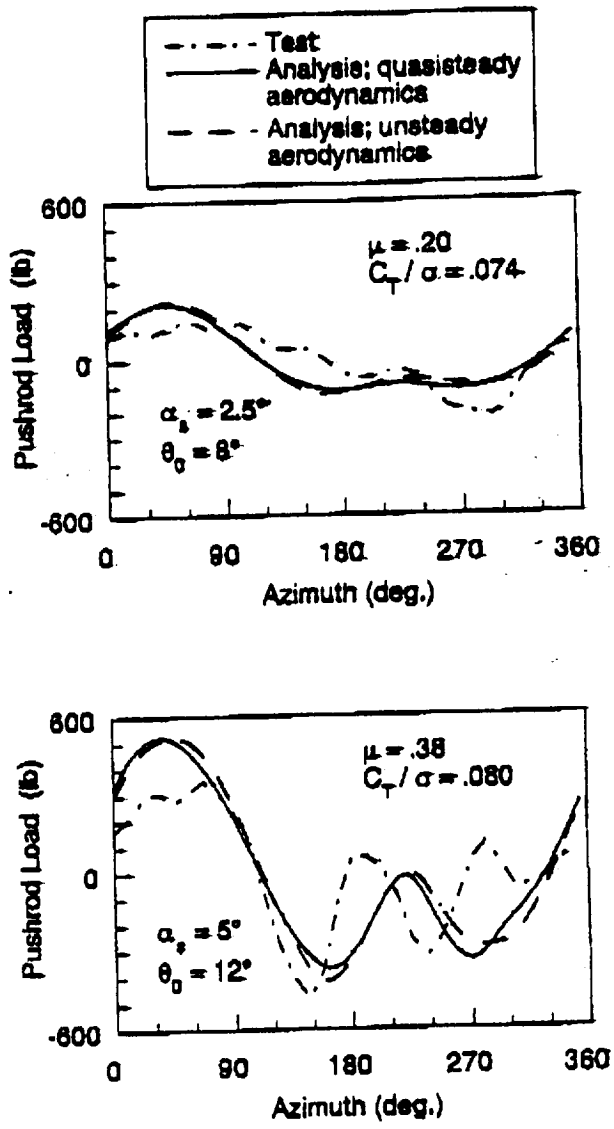

Figure 5: Measured and predicted pitch link loads.

to be a significant factor. That the data correspond to a fairly moderate values of C_T/σ also suggests that the stall model is not essential in this case.

Jepson *et. al.* (Ref. 10) conducted an extensive correlation study using data from the tests documented in Ref. 8. One conclusion of this study was that the fuselage flow field can have a significant effect on blade and pushrod loads. Based on this it appears that including flow effects of the test stand body might improve the correlation in Figure 5.

In the present analysis the control inputs are assumed to take place about the blade undeformed axis; this in essence corresponds to a hinge sequence with the feather axis inboard of both the flap and lag

hinges. However, in the subject aircraft the pitch bearing flaps and lags with the blade spindle. Also, there is a small amount of pitch-lag coupling due to the pushrod kinematics which has been neglected in the analysis. Instead of detailed tabulated airfoil data such as may be found in Refs. 8 and 9, the blade airfoil is represented in the analysis with the analytical expressions

$$c_l = c_{l_0} + c_{l_\alpha}\alpha$$
$$c_d, c_{m_{ac}} = \text{constant}$$

derived from the tabulated data near $\alpha = 0°$. Finally, it may be noted that at this operating condition the cyclic and collective pitch settings are not prescribed. The differences in the predicted and measured loads may be attributed in part to differences in predicted and actual trim controls. Neither Ref. 8 nor Ref. 10 report these data so it is difficult to make a statement regarding correlation of the trim control predictions.

In summary, it appears an actual case study of pushrod tuning for a specific aircraft would necessitate certain refinements to the analysis. However, the present investigation is more of the nature of a feasibility study; the major features of the blade torsional response, insofar as they may be affected by varying blade pushrod stiffness and damping, are well predicted. It is expected that the qualitative results of the present study will hold after refinements to the analysis have been implemented, and be valid for the subject aircraft itself.

Effect of pushrod stiffness and damping on blade dynamic characteristics

Figure 6 shows the effects of decreased pushrod stiffness on rotating blade natural frequencies. The blade dynamics are characterized by the close proximity of three strongly coupled normal modes. The modes are therefore labeled according to their mode shapes at the baseline pushrod stiffness. At very low values of pushrod stiffness, it is the low frequency branch that has the nature of a first torsional mode. As $\bar{k}_p$ is reduced to a nondimensional value of 5, this mode rapidly approaches 3/rev and the dynamics of the mode become increasingly dominated by the pushrod stiffness. Figure 7 compares the torsional mode shapes of the first torsional mode for two cases, the baseline stiffness and a reduced stiffness ($\bar{k}_p = 5$). At the lower torsional stiffness the mode begins to take on the nature of a rigid body feather mode. This is to be contrasted with changes in torsional dynamics accompanying reductions in blade torsional stiffness.

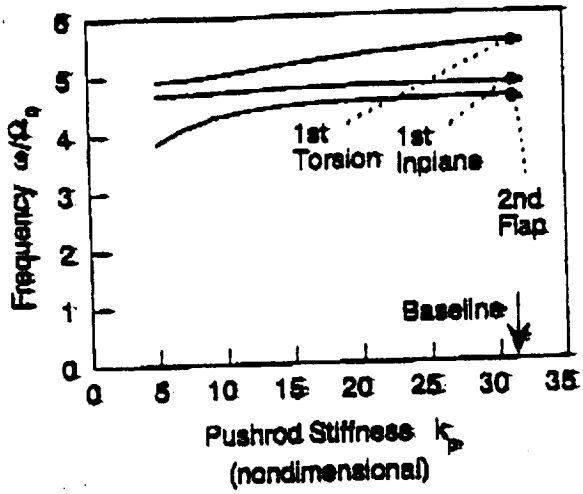

Figure 6: Effect of pushrod stiffness on blade *in-vacuo* rotating natural frequencies. Zero pushrod damping.

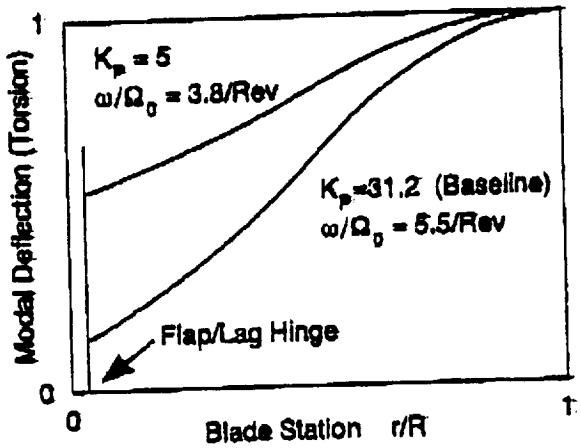

Figure 7: Effect of pushrod stiffness on blade *in-vacuo* rotating torsional mode shape. Zero pushrod damping.

In the latter case, the softness of the blade relative to the root torsional restraint causes the mode shape to become even more like that of a blade with infinitely stiff root restraint.

Figure 8 shows the effect of varying pushrod stiffness and damping on *in-vacuo* frequency and damping of the blade first torsional mode. As with Fig. 6, there are actually three modes that may be candidates for the first torsional mode. When generating Fig. 6, an attempt was made to select the mode most resembling a "pure" torsion mode. Hence, the various points on the $\bar{k}_p$-$\bar{c}_p$ map in the figure do not correspond to a single locus of frequency roots. At and above $\bar{k}_p = 20$, the damped natural frequency is very close to its baseline value of 5.5/rev. As may be

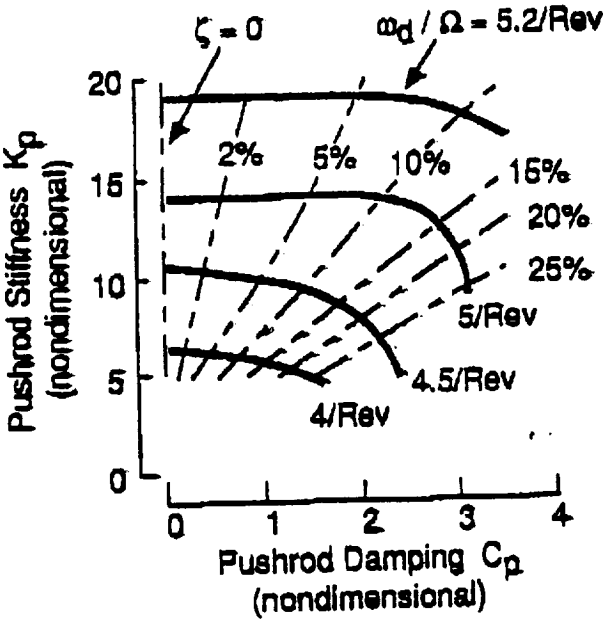

Figure 8: Effect of pushrod stiffness and damping on *in-vacuo* frequency and damping of blade first torsional mode.

expected, as the pushrod stiffness is decreased, the pushrod damping becomes more effective at increasing the damping ratio of the torsional mode. This is due to the fact that as the mode shape changes to involve more displacement at the root (Fig. 7), more energy per cycle can be dissipated through blade root damper motion. The damped natural frequency also becomes more sensitive to pushrod damping at low values of $\bar{k}_p$. The figure shows that even at the lowest values of pushrod stiffness, below $\bar{c}_p \approx 2-3$, the calculated damped frequencies are well below the rigid pushrod case, indicating that the error due to using undamped normal modes may be neglected up to these damping values (compare with Figure 4).

Effect of pushrod tuning on vibratory hub loads

Figure 9 shows the effects of blade tuning on fixed system 4/rev loads in wind tunnel trim at $\mu = .38$ (this operating condition, together with the $\mu = .20$ condition in Fig. 11, was chosen to match the conditions in the wind tunnel test described above). The forces have been normalized by $m_0\Omega^2R^2 = 57,600$ lb and the moments by $m_0\Omega^2R^3 = 1.27 \times 10^6$ ft-lb.

With zero pushrod damping, little effect is observed down to $\bar{k}_p \approx 10$, at which point the fixed system loads tend to increase with a further reduction in $\bar{k}_p$, in some cases dramatically. For reference, the point at which the first torsional frequency crosses through 4/rev is indicated with a bold symbol ("•"). Although it is the 5/rev loads which tend to increase most sharply at low pushrod stiffness, significant increases in 3 and 4/rev loads may be observed as well. At very low values of $\bar{k}_p$ the data were limited by difficulties in obtaining a trim solution. This is attributed to effects on control system effectiveness, discussed below.

With the introduction of a moderate amount of damping ($\bar{c}_p = 2$) the trends in the fixed system vibratory loads are reversed (for reference, a combination of $\bar{c}_p = 2$ and $\bar{k}_p = 5$ yields a damping ratio of just over 25% for the first torsion mode - see Fig. 8). In the case of the longitudinal inplane shear and the hub pitch and roll moments, reductions ranging from 25 to 50% over the baseline case ($\bar{k}_p = 31.2, \bar{c}_p = 0$) may be observed. A further increase of damping to $\bar{c}_p = 3$ brought little further improvement in the hub loads. Apparently most of the beneficial effects of damping are obtained with levels of damping sufficiently low that errors due to using undamped normal modes may be neglected.

The sharp increase in fixed system vibratory load in the zero damping case below $\bar{k}_p = 10$ may be observed directly in the rotating system data in Figure 10. The figure also shows that the reduction in fixed system 4/rev load at $\bar{c}_p = 3$ and $\bar{k}_p < 10$ is associated mainly with reductions in rotating system 3/rev inplane shears. The vibratory moments and the $\bar{c}_p = 2$ data have been omitted for clarity.

Figure 11 shows fixed system 4/rev hub loads for $\mu = .20$. Again at this advance ratio, favorable results may be obtained at combinations of low pushrod stiffness and moderate pushrod damping.

Note from the hub loads results that near the baseline pushrod stiffness, introduction of damping has almost no effect. Also, the large peaks in amplitude observed in the rigid blade study when operating slightly off the optimum pushrod stiffness (Fig. 2) are not present in this elastic blade data.

Influence on pushrod loads

In Figure 12, the 1 and 2/rev pushrod loads are shown as a function of pushrod stiffness for zero damping and $\bar{c}_p = 3$. At $\mu = .38$, the 1/rev pushrod load increases by around 50% as the pushrod stiffness is reduced from its baseline value to $\bar{k}_p = 5$. The 2/rev is less significantly affected but still increases by around 20%. Addition of pushrod damping seems to reduce 2/rev loads slightly; the 1/rev loads however remain virtually unaffected. These phenomenon are much less pronounced at $\mu = .2$. Here a slight improvement

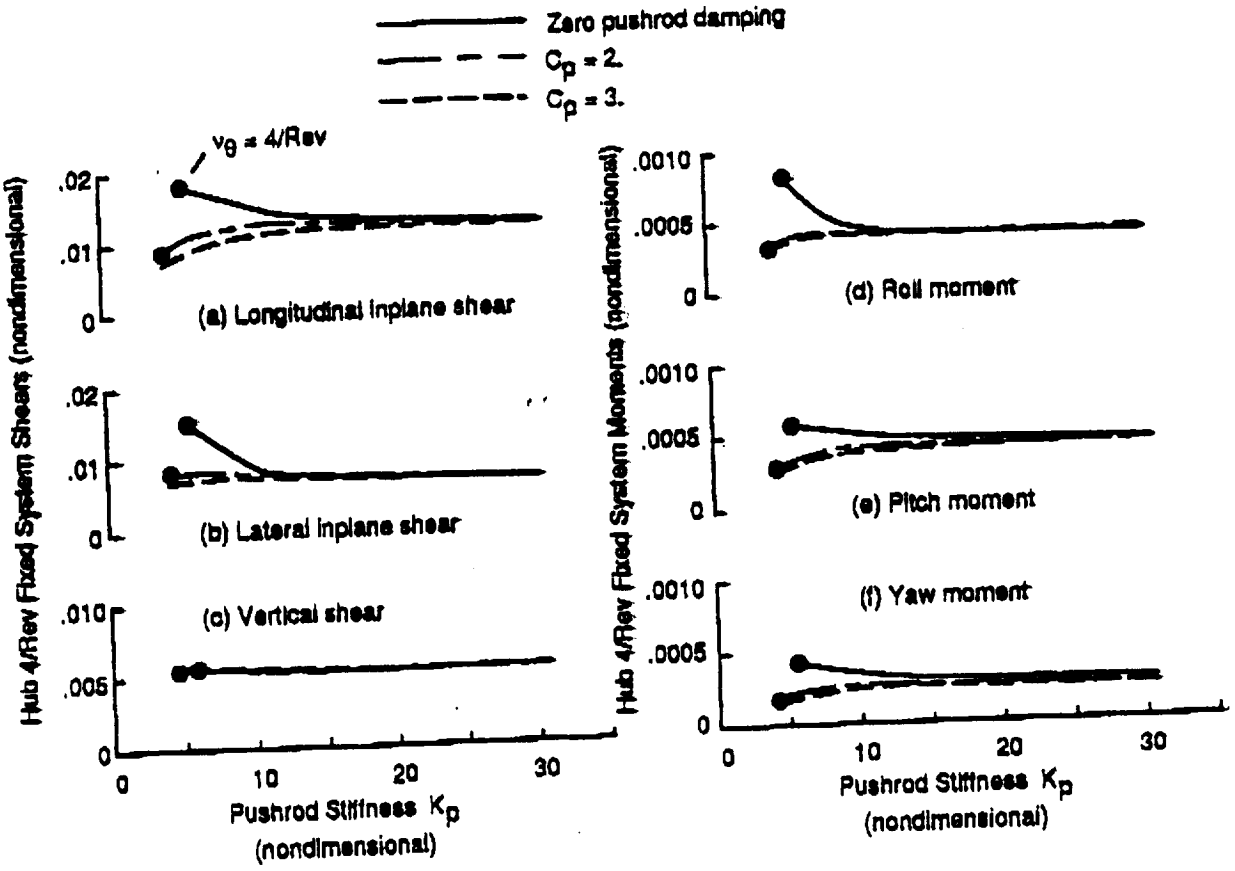

Figure 9: Fixed system 4/rev hub loads for $\mu = .38$, $C_T/\sigma = .080$, and $\alpha_s = 5°$

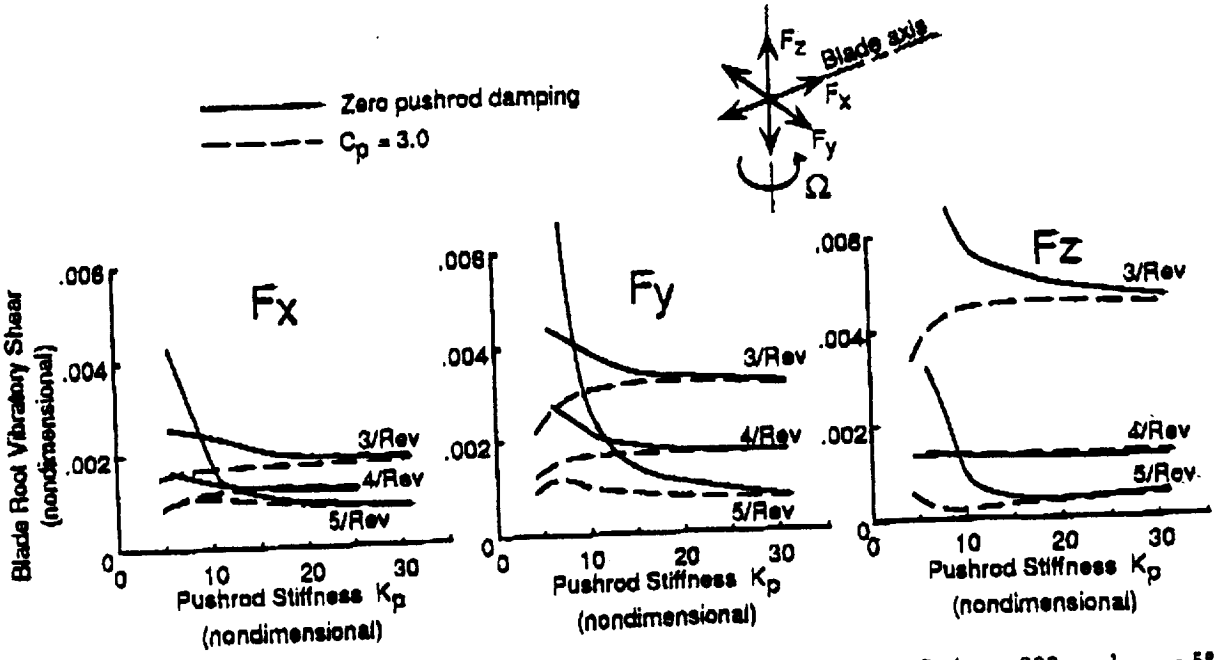

Figure 10: Rotating system 3, 4, and 5/rev blade root loads for $\mu = .38$, $C_T/\sigma = .080$, and $\alpha_s = 5°$

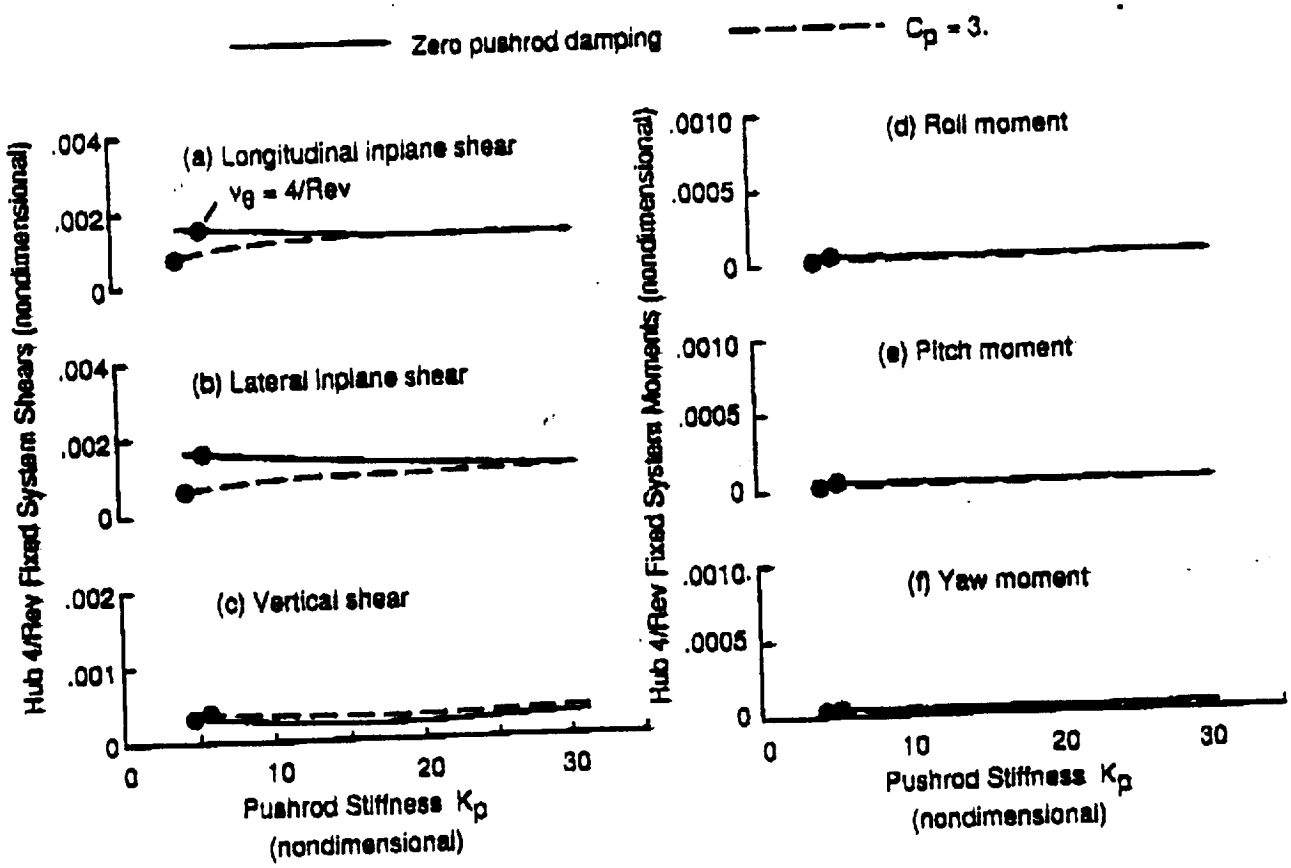

Figure 11: Fixed system 4/rev hub loads for $\mu = .20$, $C_T/\sigma = .074$, and $\alpha_s = 2.5°$

in 2/rev loads at low values of $\bar{k}_p$ may be observed.

The large increase in vibratory pushrod loads at low pushrod stiffness at $\mu = .38$ is significant. Although the pushrod itself would be replaced by an entirely new component sized to handle these vibratory loads, the pushrod loads have implications for loads in other control system components such as the swashplate and servos. It is envisioned that the device may be retrofitted to existing aircraft; this advantage of ease of application disappears if other control system components require redesign or reduced time to replacement.

The hub loads shown in this study were obtained using a force summation method; no distinction is made between loads reacted through the hub and loads reacted through the pushrod. This distinction, however, is of potential interest. The vibratory pushrod load feeds into the fixed system through the non-rotating part of the control system. Changes in hub loads may have a different effect on fuselage vibration depending on whether they are reacted through the rotor shaft or through the pushrod. To properly capture this effect would require the fuselage and nonrotating control system to be modeled in some detail. (See also Refs. 11 and 12 for a discussion of the effects of control loads on fuselage vibrations.)

Effect on trim control settings

Figure 13 shows the effects of pushrod tuning on trim control positions. At both $\mu = .20$ and $\mu = .38$, reduced pushrod stiffness seems to have little effect on collective pitch required. An increase in forward longitudinal cyclic is present, especially at $\mu = .38$. Of particular interest is the trend of lateral cyclic at $\mu = .38$. At very low values of $\bar{k}_p$, the lateral cyclic drifts by about 5°; at around $\bar{k}_p = 8$ it actually changes sign. This is probably why difficulties were encountered when finding the trim solution at very low values of pushrod stiffness. In the present analysis, the control positions are adjusted to yield zero first harmonic flapping using a tangential matrix obtained from a rigid blade model. Apparently the reduced pushrod stiffness brings about a phase delay in the blade flapping response, changing the system response to cyclic pitch in such a way that the rigid blade tangential matrix no longer guarantees

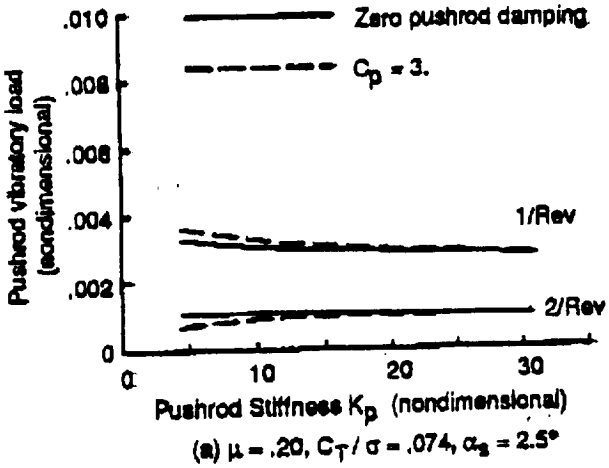

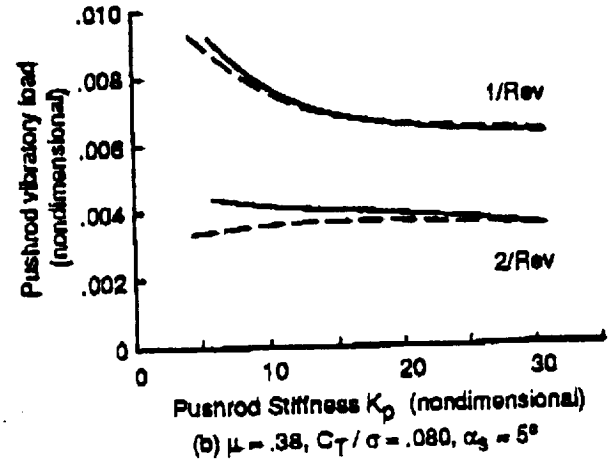

Figure 12: Pushrod loads.

trim convergence. Introduction of pushrod damping alleviates this situation. Difficulties in finding a trim solution may also arise from actual instabilities introduced by reducing the pushrod stiffness (aeromechanical stability was not examined in this investigation) Pushrod tuning may or may not have a significant effect on trim controls of a free flying aircraft. The present investigation was limited to the wind tunnel trim case in order to match the test operating conditions in Ref. 8.

Practical implementation

Regarding a practical implementation of a spring-damper pushrod with desireable stiffness and damping values as identified in this study, consider the devices described in Ref. 4. They provide useful data points as to what dynamic properties are possible with such a device. The pushrods had a spring rate of 5000 lb/in and a damping rate of 90 lb-sec/in. These values may be nondimensionalized in the present scheme with

$$\bar{k}_p = 60{,}000 \text{ lb/ft} \div m_0\Omega^2 R \approx 23$$
$$\bar{c}_p = 1080 \text{ slug/sec} \div m_0\Omega R \approx 13$$

Presumably the damping rate could be arbitrarily reduced to the desired value of $\bar{c}_p \approx 2-3$ by modification of the orifice size. More difficulty may be encountered achieving the low spring rate required ($\bar{k}_p \approx 5$). In Ref. 4, elastomeric elements were used to provide the required compliance. This suggests an integrated elastomeric spring-damper pushrod. Possibly the required damping can be provided by the elastomer itself, eliminating the need for a hydraulic damper.

Summary and Conclusions

The possibilities for vibration reduction with a dynamically tuned main rotor blade pushrod has been examined analytically. This device could be a direct replacement for blade pushrods on new or existing aircraft.

1. A parametric study indicates that vibratory hub loads are severely degraded with very low values of pushrod stiffness and no pushrod damping. However, combinations of reduced pushrod stiffness and moderate damping yielded fixed system 4/rev hub loads which in some cases were reduced by up to 50% of their baseline values. The pushrod 1/rev loads, however, increased by about 50%.

2. The agreement between pushrod loads predicted by the analysis and those measured experimentally is fair. There is a reasonable expectation that this correlation may improve with refinements to the analysis such as introduction of a free wake model and improved modeling of blade root kinematics.

3. With no damping, reduced pushrod stiffness may have a significant effect on trim controls.

4. Since the pushrod damper represents a change in boundary condition, errors may be introduced when a modal reduction is applied using undamped normal modes. However, this does not appear to be a problem for the values of pushrod damping considered in this study.

5. Further test and analytic work is recommended. The beneficial effects of pushrod tuning need to

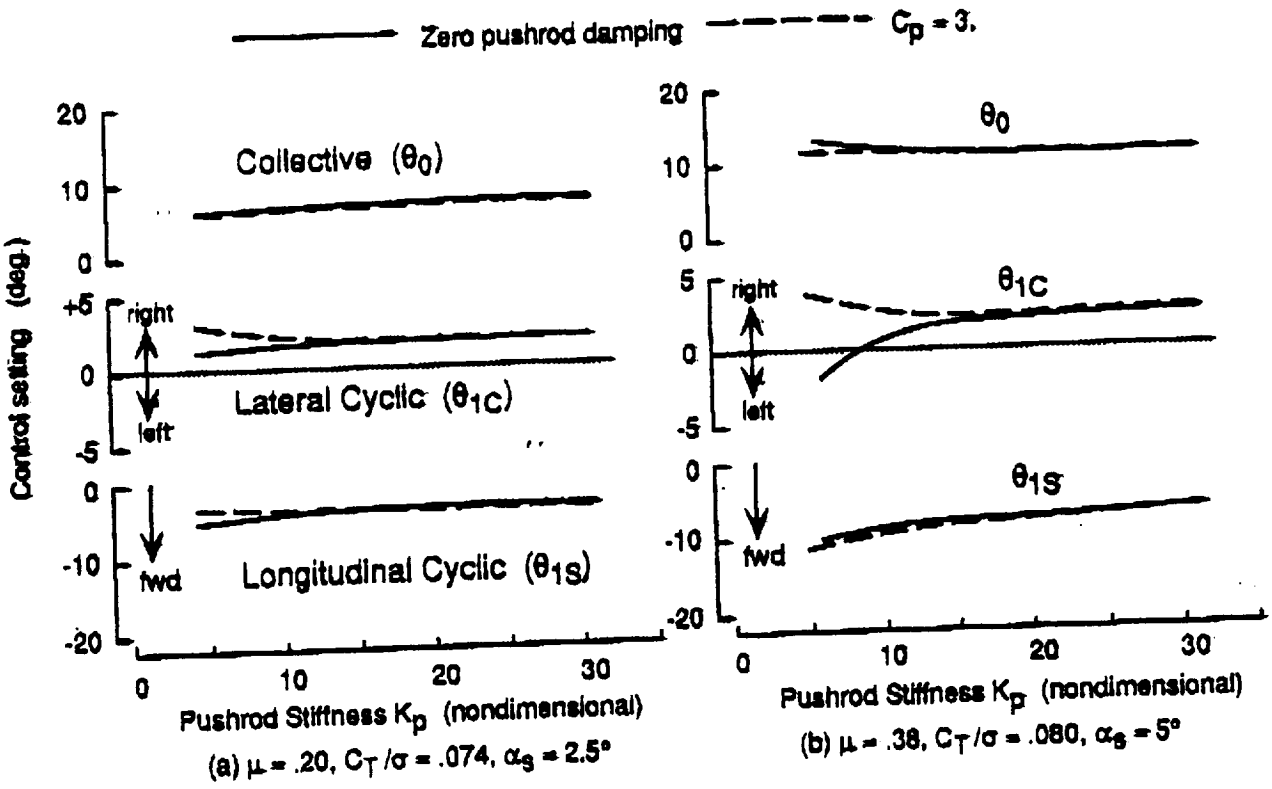

Figure 13: Trim controls.

be confirmed experimentally. Attention should be given to the effects of pushrod tuning on aeromechanical stability, handling qualities, and blade dynamic stall behavior. Other issues which should be addressed in future investigations are (1) effects on handling qualities (trim control gradients; maneuver response) and (2) effects on dynamic stall behavior at conditions of high rotor loading.

References

[1]Miller, R. H. and Ellis, C. W., "Helicopter Blade Vibration and Flutter," *Journal of the American Helicopter Society*, Vol. 1, (3), July 1956.

[2]Tarzanin, F. J. and Ranieri, J., "Investigation of the Effect of Torsional Natural Frequency on Stall-Induced Dynamic Loading," USAAMRDL Technical Report 73-94; NTIS N74-25544, February 1974.

[3]Gabel, R. and Tarzanin, F. J., "Blade Torsional Tuning to Manage Large Amplitude Control Loads," *Journal of Aircraft*, Vol. 11, (8), August 1974.

[4]Nettles, W. E., Paul, W. F., and Adams, D. O., "Evaluation of a Stall-Flutter Spring-Damper Pushrod in the Rotating Control System of a CH-54B Helicopter," Presented at the AHS/NASA-Ames Specialists' Meeting on Rotorcraft Dynamics, February 1974.

[5]Kottapalli, S., "Blade Root Torsional Dampers to Reduce Hub Loads," AIAA 33rd Structures, Structural Dynamics, and Materials Conference, Dallas, Texas. Paper AIAA-92-2449, April 1992.

[6]Den Hartog, J. P., *Mechanical Vibrations*, Dover, New York, 1985.

[7]Bir, G., Chopra, I., et al., "University of Maryland Advanced Rotor Code (UMARC) Theory Manual," UM-AERO 92-02, University of Maryland, College Park, Maryland, November 1991.

[8]Johnson, W., "Performance and Loads Data from a Wind Tunnel Test of a Full-Scale Rotor with Four Blade Tip Planforms," NASA TM-81229; USAAVRADCOM TR 80-A-9, 1980.

[9]Kottapalli, S. and Leyland, J., "Analysis of Open Loop Higher Harmonic Control at High Airspeeds on a Modern Four-Bladed Articulated Rotor," NASA TM 103876, August 1991.

[10]Jepson, D., Moffitt, R., Hilsinger, K., and Bissell, J., "Analysis and Correlation of test Data From an Advanced Technology Rotor System," NASA-CR 3714, August 1983.

[11]Kidd, D., Spivey, R., and Lawrence, K., "Control Loads and Their Effects on Fuselage Vibrations," *Journal of the American Helicopter Society*, Vol. 12, (4), October 1967.

[12]Mard, K. C., "Comments on "Effects of Control Loads on Fuselage Vibration by D. Kidd, R. Spivey, K. Lawrence"," *Journal of the American Helicopter Society*, Vol. 12, (4), October 1967.